2007

Epitaxial lateral overgrowth of (112¯2) semipolar GaN on (11¯00) m-plane sapphire by metalorganic chemical vapor deposition

X. Ni
Virginia Commonwealth University, nix@vcu.edu

Ü. Özgür
Virginia Commonwealth University, uozgur@vcu.edu

A. A. Baski
Virginia Commonwealth University, aabaski@vcu.edu

See next page for additional authors

Ni, X., Özgür, Ü., Baski, A.A., et al. Epitaxial lateral overgrowth of (112¯2) semipolar GaN on (11¯00) m-plane sapphire by metalorganic chemical vapor deposition. Applied Physics Letters, 90, 182109 (2007).

Epitaxial lateral overgrowth of $(11\bar{2}2)$ semipolar GaN on $(1\bar{1}00)$ *m*-plane sapphire by metalorganic chemical vapor deposition

X. Ni,[a] Ü. Özgür, A. A. Baski, and H. Morkoç
Department of Electrical and Computer Engineering, Virginia Commonwealth University, Richmond, Virginia 23284 and Department of Physics, Virginia Commonwealth University, Richmond, Virginia 23284

Lin Zhou and David J. Smith
Department of Physics, Arizona State University, Tempe, Arizona 85287

C. A. Tran
SemiLEDs, Semi-Photonics Co. Ltd., Hsinchu Science Park, Chu-Nan 3350, Miao-Li County, Taiwan, Republic of China

(Received 29 December 2006; accepted 8 April 2007; published online 2 May 2007)

The authors report the growth of semipolar $(11\bar{2}2)$ GaN films on nominally on-axis $(10\bar{1}0)$ *m*-plane sapphire substrates using metal organic chemical vapor deposition. High-resolution x-ray diffraction (XRD) results indicate a preferred $(11\bar{2}2)$ GaN orientation. Moreover, epitaxial lateral overgrowth (ELO) of GaN was carried out on the $(11\bar{2}2)$ oriented GaN templates. When the ELO stripes were aligned along $[11\bar{2}0]_{\text{sapphire}}$, the Ga-polar wings were inclined by 32° with respect to the substrate plane with smooth extended nonpolar *a*-plane GaN surfaces and polar *c*-plane GaN growth fronts. When compared with the template, the on-axis and off-axis XRD rocking curves indicated significant improvement in the crystalline quality by ELO for this mask orientation (*on-axis* 1700 arc sec for the template, 380 arc sec for the ELO sample, when rocked toward the GaN *m* axis), as verified by transmission electron microscopy (TEM). For growth mask stripes aligned along $[0001]_{\text{sapphire}}$ with GaN *m*-plane as growth fronts, the surface was composed of two $\{10\bar{1}1\}$ planes making a 26° angle with the substrate plane. For this mask orientation XRD and TEM showed no improvement in the crystalline quality by ELO when compared to the non-ELO template. © *2007 American Institute of Physics*. [DOI: 10.1063/1.2735558]

Growth of GaN films oriented along nonpolar and semipolar directions of GaN have been receiving considerable attention to alleviate the spontaneous and strain-induced piezoelectric polarization effects that are inherent to the *c*-axis-oriented hexagonal GaN system.[1] Among the two common nonpolar planes of GaN, the *a*-plane GaN can be grown on *r*-plane sapphire using molecular beam epitaxy,[2] or metal organic chemical vapor deposition (MOCVD).[3,4] However, the development of *a*-plane GaN has been hindered by its low crystalline quality even with epitaxial lateral overgrowth (ELO), mainly due to the low formation energy of basal-plane stacking faults (BSFs).[5,6] The *m*-plane GaN can currently only be obtained on γ-$LiAlO_2$ (100) (Ref. 7) and *m*-plane SiC substrates,[8] which both have limited availability and higher cost compared with sapphire. Employing semipolar GaN is another option to reduce polarization effects. $(10\bar{1}3)$ or $(11\bar{2}2)$ oriented semipolar GaN has been grown on *m*-plane sapphire using hydride vapor phase epitaxy (HVPE),[9] and electroluminescence from semipolar InGaN/GaN light emitting diodes has showed a reduced blueshift with increasing drive current compared to the *c*-plane counterparts, indicative of reduced polarization in the active layer.[10] However, no systematic study of semipolar GaN growth by MOCVD on nominal *m*-plane sapphire has been reported. In this letter, we describe a detailed investigation of GaN growth on *m*-plane sapphire using MOCVD, which could also provide a better understanding of GaN growth on nonpolar sapphire substrates, and ultimately help to realize high material quality in this orientation.

GaN films investigated in this study were grown on nominally on-axis $(10\bar{1}0)$ *m*-plane sapphire substrates [less than 0.1° miscut as measured by x-ray diffraction (XRD)] using MOCVD. Trimethylgallium (TMGa) and ammonia were used as the Ga and N sources, respectively. Following *in situ* annealing of the chemically cleaned sapphire substrate, a 45-nm-thick low-temperature GaN nucleation layer was deposited at 550 °C. The temperature was then raised to 1030 °C for the subsequent growth of a 1.2-μm-thick GaN epilayer. The ELO of GaN on *m*-plane sapphire was also carried out using $(11\bar{2}2)$ GaN films as the template. The growth mask was a 140-nm-thick SiO_2 layer deposited using plasma-enhanced chemical vapor deposition. A mask pattern with 10-μm-wide stripes and 4-μm-wide windows was transferred onto two different pieces of the template using standard lithographic procedures: one having stripes oriented along the $[1\bar{2}10]$ *a* axis and the other along the [0001] *c* axis of the sapphire substrate. The two samples were grown side by side under identical conditions in the MOCVD chamber. The flow rates of TMGa and NH_3 were kept at 117 μmol/min and 550 SCCM (SCCM denotes cubic centimeter per minute at STP), respectively, with the growth pressure at 30 Torr. The growth time was kept short (1 h) and coalescence of the wings was avoided so that advancement of the growth fronts could be observed.

To determine the crystallographic orientation and the crystalline quality, the as-grown GaN films on *m*-plane sap-

[a]Electronic mail: nix@vcu.edu

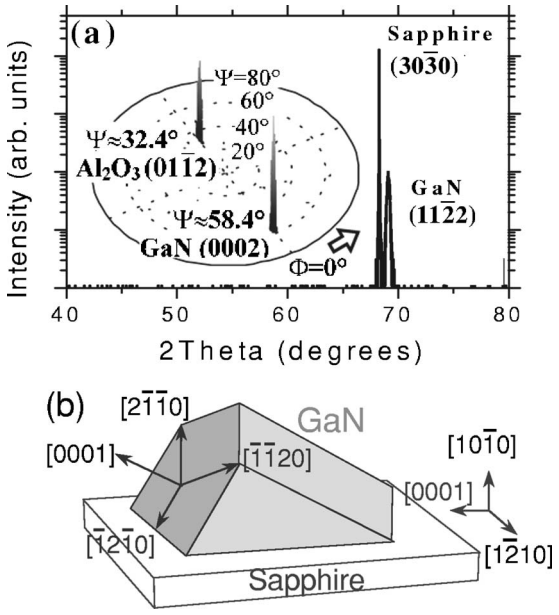

FIG. 1. (a) XRD 2θ-ω scan for GaN grown on *m*-plane sapphire, with the inset showing the *off-axis* ϕ scans with different ψ tilt angles (i.e., pole figure) for GaN (0002) and sapphire (01$\bar{1}$2) of GaN (11$\bar{2}$2) on *m*-plane sapphire. (b) A schematic depicting the epitaxial relationship derived from XRD measurements for (11$\bar{2}$2) GaN on *m*-plane sapphire.

phire were characterized by high-resolution XRD. As shown in Fig. 1(a), on-axis 2θ-ω scans indicate that the surface orientation is $(11\bar{2}2)_{GaN}\|(10\bar{1}0)_{sapphire}$. The full width at half maximum (FWHM) values of XRD rocking curves for the on-axis GaN (11$\bar{2}$2) and off-axis GaN(0002) shown in Table I for different rocking directions are similar to those reported for GaN films grown on *m* sapphire using HVPE (see also Table I). However, unlike the case of HVPE, no (10$\bar{1}\bar{3}$) oriented GaN films were obtained even after high-temperature nitridation of the sapphire substrate in NH_3 (550 SCCM) atmosphere at 1030 °C for 2 min or an increase of NH_3 flow rate (from 550 to 7060 SCCM) during the initial stages of the epitaxial growth.

In order to obtain the in-plane epitaxial relationship, off-axis ϕ scans were performed at different ψ tilt angles for the (11$\bar{2}$2) GaN film. From the pole figure in Fig. 1(a) inset, it is concluded that $(0002)_{GaN}$ is oriented 180° away from

TABLE I. FWHM values (in arc sec) of XRD rocking curves for (11$\bar{2}$2) GaN templates, ELO samples with mask stripes along the *a* axis and *c* axis of sapphire, and an *a*-plane GaN ELO sample for different rocking directions.

XRD reflection/rocking direction	GaN (11$\bar{2}$2) templates		ELO GaN (11$\bar{2}$2) stripes along sapphire's	
	This work	By HVPE[a]	*a* axis	*c* axis
(11$\bar{2}$2)/*m* axis	1700	1500	380	1800
(11$\bar{2}$2)/*c* axis	1100	1400	610	1300
(0002)	2400	2200	350	···
(11$\bar{2}$0)/*m* axis	···	···	380 (760[b])	···
(10$\bar{1}$1)/*c* axis	···	···	···	1700

[a]Reference 9.
[b]GaN (11$\bar{2}$0) ELO sample (Ref. 13).

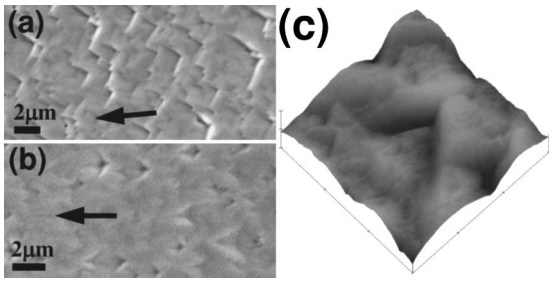

FIG. 2. Plan-view SEM images of GaN samples grown on *m*-plane sapphire using an NH_3 flow rate of (a) 550 and (b) 7060 SCCM for the first 10 min and 550 SCCM for the rest of the growth. The arrows indicate the *c* axis of sapphire. (c) A 3D AFM image (3×3 μm^2) of a V-shaped surface feature (Δz=150 nm).

$(01\bar{1}2)_{sapphire}$. The GaN (11$\bar{2}$2) plane forms an angle of 58.4° with $(0002)_{GaN}$; while the sapphire (01$\bar{1}$2) plane forms an angle of 32.4° with the sapphire (10$\bar{1}$0) *m* plane. After combining these results, one determines the epitaxial relationships for GaN on *m*-plane sapphire, as shown in Fig. 1(b), namely, $(11\bar{2}2)_{GaN}\|(10\bar{1}0)_{sapphire}$, $[10\bar{1}0]_{GaN}\|[1\bar{2}10]_{sapphire}$, and $[1\bar{2}1\bar{1}]_{GaN}\|[0001]_{sapphire}$.

Fig. 2(a) shows a plan-view scanning electron microscopy (SEM) image of the GaN (11$\bar{2}$2) film grown using 550 SCCM NH_3 flow rate as described above. The image is indicative of a rough surface with "V-shaped" features (with pits placed at the corners) that are oriented along the *c* direction of the sapphire substrate. Although the orientation of the GaN films was not sensitive to the growth conditions in this study, the surface morphology of the samples exhibited slightly different features under different growth conditions, especially with changing ammonia flow rate. Based on the growth conditions for the sample shown in Fig. 2(a), when the NH_3 flow rate was changed from 550 to 7060 sccm for the first 10 min of the epilayer growth, different surface features were observed, as shown in Fig. 2(b). The pits in this image are surrounded by four facets, two of which make an angle of approximately 110°, which is similar to the V-shaped features in Fig. 2(a), while the other two make an angle of approximately 50°. The facets for the V-shaped features or pits seem to be the GaN {10$\bar{1}$1} planes, which are very stable and often observed during MOCVD growth of *c*-plane and *a*-plane GaN.[11,12] The angle between the two neighboring {10$\bar{1}$1} planes is 127.6° which would be observed as 113° or 50° when projected onto the GaN (11$\bar{2}$2) surface, consistent with the figures measured from the SEM images in Fig. 2. The observed angle values, however, show a wide distribution between 90° and 115°, most probably due to the varying amount of deposition on these planes. The structure of the V-shaped feature is clearly seen in the three-dimensional (3D) atomic force microscopy (AFM) image of Fig. 2(c).

In order to reduce the extended defect density and also to study the lateral growth behavior of this semipolar film, ELO was carried out on a (11$\bar{2}$2) GaN template (grown using 550 sccm NH_3) with the stripe orientations described above. Fig. 3(a) shows a plan-view SEM image for the ELO sample with SiO_2 stripes oriented along the *a* axis of the sapphire substrate. It is clear from the cross-sectional SEM image in Fig. 3(b) that the wings for this mask orientation are inclined

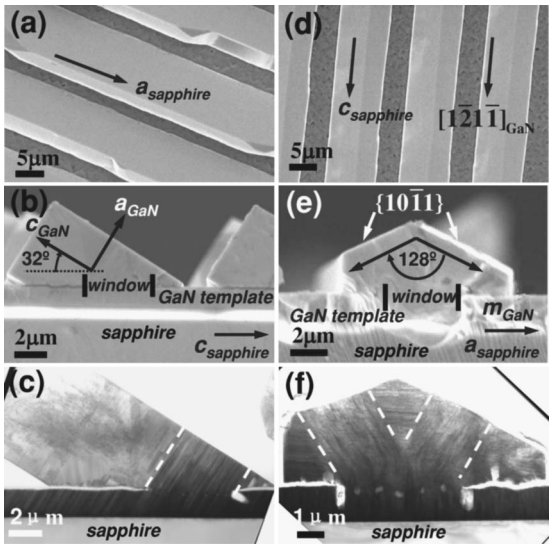

FIG. 3. (a) Plan-view SEM, (b) cross-sectional SEM, and (c) cross-sectional TEM images of GaN ELO sample with SiO_2 stripes oriented along the *a* axis of sapphire. (d) Plan-view SEM, (e) cross-sectional SEM, and (c) cross-sectional TEM images of the GaN ELO sample with SiO_2 stripes oriented along the *c* axis of sapphire.

by 32° with respect to the substrate plane with well-defined *a*- and *c*-plane surfaces. The growth along the *c* axis advances faster than that in other directions; therefore, the observation of inclined wings is consistent with the epitaxial relationships shown in Fig. 1, which suggest a 32.4° angle between the *c* axis of GaN and *c* axis of sapphire. The upwardly inclined wings are tentatively attributed to the Ga-polar (0001) wings, since their growth fronts (GaN *c* plane) are smooth with rare occurrences of some facets as observed in the SEM images, while the N-polar (000$\bar{1}$) surfaces often feature hexagonal hillocks.[12] Because of the large incline angle, only the Ga-polar wings extend while the N-polar wing growth is stymied by the template. With further growth on this ELO sample, the Ga-polar wings extended further along the *c* axis of GaN with negligible growth along the *a* axis. Unlike the GaN (11$\bar{2}$2) surface of the template shown in Fig. 2, both *a*- and *c*-plane surfaces of the wings are very smooth. AFM measurements on the *a*-plane surfaces of the wings revealed no striated features along the *c* axis that are characteristic of the *a*-plane GaN growth on *r*-plane sapphire,[4] and a root-mean-square surface roughness of ~2 nm, which is much smaller than that of the fully coalesced *a*-plane GaN ELO layers (9–15 nm).[13] This would suggest a promising route for the growth of high-quality nonpolar GaN.

Compared to the (11$\bar{2}$2) GaN templates on *m*-plane sapphire and also *a*-plane GaN ELO samples,[13] significant improvement of the crystalline quality has been achieved with ELO, as exemplified by the XRD rocking curve data summarized in Table I. The FWHM values of the XRD rocking curves for the on-axis GaN (11$\bar{2}$2) after ELO were reduced to 380 and 610 arc sec when rocked toward the GaN *m* axis and *c* axis, respectively. This suggests significant reduction in the defect density,[14] as confirmed by the cross-sectional transmission electron microscopy (TEM) image shown in Fig. 3(c). The high number of BSFs that appear in the template and also in the window regions are effectively eliminated in the overgrown Ga wings, which exhibit an average dislocation density of only $\sim 10^7$ cm^{-2}.

For the second ELO sample, the SiO_2 mask stripes were oriented along the *c* axis of the sapphire substrate, which is also along GaN [1$\bar{2}$1$\bar{1}$]. In this stripe orientation, the lateral overgrowth should progress along the *m* axis of GaN. Figure 3(d) shows the plan-view SEM image for this ELO sample. The cross-sectional SEM image in Fig. 3(e) indicates the formation of two different planes that make an angle of 26° with the substrate plane. Using XRD studies these surfaces were identified as {10$\bar{1}$1}. According to the XRD rocking curve results shown in Table I, no improvement of the crystal quality is achieved for this stripe orientation when compared to the (11$\bar{2}$2) GaN templates on *m*-plane sapphire and the ELO sample with SiO_2 stripes oriented along the *a* axis of the sapphire. From the cross-sectional TEM image of this sample [see Fig. 3(f)], it is evident that the BSFs (observed as horizontal lines which represent the cross section of these planar defects with the [1$\bar{2}$1$\bar{1}$] plane of GaN) cannot be blocked but propagate laterally in the overgrown material for this particular stripe orientation. In addition, the threading dislocations originating from the template bend towards the two {10$\bar{1}$1} surfaces and are partially eliminated only in a very limited part of the overgrown volume. Therefore, both XRD and TEM results suggest that no significant dislocation density reduction occurs when the stripes in the mask are oriented along the *c* axis of sapphire.

In summary, significant improvement of the crystalline quality was achieved by ELO with a relatively small amount of overgrowth only when the mask stripes were oriented along the sapphire *a* axis according to the XRD rocking curve and TEM measurements.

This work was supported by Air Force Office of Scientific Research under the direction of K. Reinhardt. The authors would like to thank Y. Fu, J. Xie, and N. Biyikli for general discussions on MOCVD.

[1]T. Deguchi, K. Sekiguchi, A. Nakamura, T. Sota, R. Matsuo, S. Chichibu, and S. Nakamura, Jpn. J. Appl. Phys., Part 2 **38**, L914 (1999).
[2]H. M. Ng, Appl. Phys. Lett. **80**, 4369 (2002).
[3]M. D. Craven, S. H. Lim, F. Wu, J. S. Speck, and S. P. DenBaars, Appl. Phys. Lett. **81**, 469 (2002).
[4]X. Ni, Y. Fu, Y. T. Moon, N. Biyikli, and H. Morkoç, J. Cryst. Growth **290**, 166 (2006).
[5]Z. Liliental-Weber, D. Zakharov, B. Wagner, and R. F. Davis, Proc. SPIE **6121**, 612101 (2006).
[6]D. Hull and D. J. Bacon, *Introduction to Dislocation*, 3rd ed. (Pergamon, Oxford, 1984), Chap. 6, p. 102.
[7]Y. J. Sun, O. Brandt, and K. H. Ploog, J. Vac. Sci. Technol. B **21**, 1350 (2003).
[8]N. F. Gardner, J. C. Kim, J. J. Wierer, Y. C. Shen, and M. R. Krames, Appl. Phys. Lett. **86**, 111101 (2005).
[9]T. J. Baker, B. A. Haskell, F. Wu, J. S. Speck, and S. Nakamura, Jpn. J. Appl. Phys., Part 2 **45**, L154 (2006).
[10]R. Sharma, P. M. Pattison, and H. Masui, R. M. Farrell, T. J. Baker, B. A. Haskell, F. Wu, S. P. DenBaars, J. S. Speck, and S. Nakamura, Appl. Phys. Lett. **87**, 231110 (2005).
[11]P. Gibart, Rep. Prog. Phys. **67**, 667 (2004).
[12]F. Wu, M. D. Craven, S. Lim, and J. S. Speck, J. Appl. Phys. **94**, 942 (2003).
[13]X. Ni, Ü. Özgür, Y. Fu, N. Biyikli, J. Xie, A. A. Baski, H. Morkoç, and Z. Liliental-Weber, Appl. Phys. Lett. **89**, 262105 (2006).
[14]B. Heying, X. H. Wu, S. Keller, Y. Li, D. Kapolnek, B. P. Keller, S. P. DenBaars, and J. S. Speck, Appl. Phys. Lett. **68**, 643 (1996).